The Astronomical Journal, 158:209 (6pp), 2019 November https://doi.org/10.3847/1538-3881/ab4c3e

In the Presence of a Wrecking Ball: Orbital Stability in the HR 5183 System

Stephen R. Kane[1] and Sarah Blunt[2,3,4]
[1] Department of Earth and Planetary Sciences, University Of California, Riverside, CA 92521, USA; skane@ucr.edu
[2] Cahill Center for Astronomy & Astrophysics, California Institute of Technology, Pasadena, CA 91106, USA
[3] Center for Astrophysics, Harvard & Smithsonian, Cambridge, MA 02138, USA
Received 2019 August 27; revised 2019 September 28; accepted 2019 October 7; published 2019 October 31

Abstract

Discoveries of exoplanets using the radial velocity method are progressively reaching out to increasingly longer orbital periods as the duration of surveys continues to climb. The improving sensitivity to potential Jupiter analogs is revealing a diversity of orbital architectures that are substantially different from that found in our solar system. An excellent example of this is the recent discovery of HR 5183b: a giant planet on a highly eccentric ($e = 0.84$) ~75 yr orbit. The presence of such giant planet orbits are intrinsically interesting from the perspective of the dynamical history of planetary systems, and also for examining the implications of ongoing dynamical stability and habitability of these systems. In this work, we examine the latter, providing results of dynamical simulations that explore the stable regions that the eccentric orbit of the HR 5183 giant planet allows to exist within the habitable zone (HZ) of the host star. Our results show that, despite the incredible perturbing influence of the giant planet, there remain a narrow range of locations within the HZ where terrestrial planets may reside in long-term stable orbits. We discuss the effects of the giant planet on the potential habitability of a stable terrestrial planet, including the modulation of terrestrial planet eccentricities and the periodically spectacular view of the giant planet from the terrestrial planet location.

Unified Astronomy Thesaurus concepts: Astrobiology (74); Exoplanets (498); Orbital evolution (1178); Habitable planets (695); Habitable zone (696); Elliptical orbits (457)

1. Introduction

As both the time baseline and precision of radial velocity (RV) instruments improve, detections of increasingly longer period planets are occurring (Wright et al. 2008; Wittenmyer et al. 2011, 2016; Kane et al. 2019). The importance of discovering such long-period giant planets is placing of our solar system architecture in context via measuring occurrence rates of Jupiter analogs (Boisse et al. 2012; Wittenmyer et al. 2013; Kipping et al. 2016; Buchhave et al. 2018), the influence of giant planets beyond the snow line on terrestrial planet habitability (Raymond 2006; Horner & Jones 2008; Georgakarakos et al. 2018; Hill et al. 2018; Sánchez et al. 2018), and possible targets for direct imaging observations (Lannier et al. 2017; Kane et al. 2018). A further investigative process that is invoked in the context of long-period planets is the exploration of orbital eccentricity distributions (Kane et al. 2012; Kipping 2013), which in turn relates to the dynamical histories of systems with eccentric planets (Kane & Raymond 2014; Carrera et al. 2016). The discovery of particularly long-period giant planets with exceptionally eccentric orbits thus present opportunities to study critical aspects of exoplanetary dynamical and habitable evolution.

The most extreme such case detected thus far using the RV method is that of HR 5183b (Blunt et al. 2019). The host star (alias HD 120066) is a slightly evolved G0 star located at a distance of 31.49 pc. The planet has one of the longest orbital periods known among exoplanets of ~75 yr and orbits the star with an eccentricity of $e = 0.84$. Despite the long orbit, the detection of RV variations during the periastron passage allowed for the confirmation of the discovery. Although no other planets have yet been detected in the system, it is useful to explore if orbits interior to the giant planet can retain their long-term dynamical integrity. The long period of the giant planet combined with the relatively high eccentricity of the orbit means that the planet could be aptly described as a wrecking ball, with its gravitational influence cyclically permeating throughout the system. A system that consists of a combination of the known planet and terrestrial planets within the star's habitable zone (HZ) would be a remarkable test case for the effects of extreme planetary orbits on the overall architecture and habitability of such systems.

Here we provide a study of the HR 5183 system that includes calculations of the HZ, dynamical simulations that scan possible stable orbit locations for additional terrestrial planets, and a discussion of the implications of extreme orbital architectures. This study addresses the question: does the presence of the wrecking ball planet pose a significant threat to orbital stability of any potentially habitable planets in the system? In Section 2 we describe the architecture of the system, including possible formation scenarios, and calculate the extent of the system HZ. Section 3 provides the details of an extensive dynamical simulation that explores regions of stability with the HZ. These simulations lead to predictions of where terrestrial planets may possibly reside, described in Section 4, including an extended discussion of potentially habitable conditions for such planets under the influence of the known giant planet. We provide concluding remarks and suggestions for further investigations in Section 5.

2. System Architecture and Habitable Zone

The full details of the HR 5183b orbit are provided by Blunt et al. (2019). The relevant properties for our dynamical analysis are the stellar mass ($M_\star = 1.07 \pm 0.04\,M_\odot$), planet mass ($M_p \sin i = 3.23^{+0.07}_{-0.06}\,M_J$), semimajor axis ($a = 18 \pm 2$ au), orbital eccentricity ($e = 0.84 \pm 0.02$), and argument of periastron ($\omega = 339.^\circ4 \pm 0.^\circ8$). Note that the planet mass is a minimum mass depending on orbital inclination. These parameters result in

[4] NSF Graduate Research Fellow.

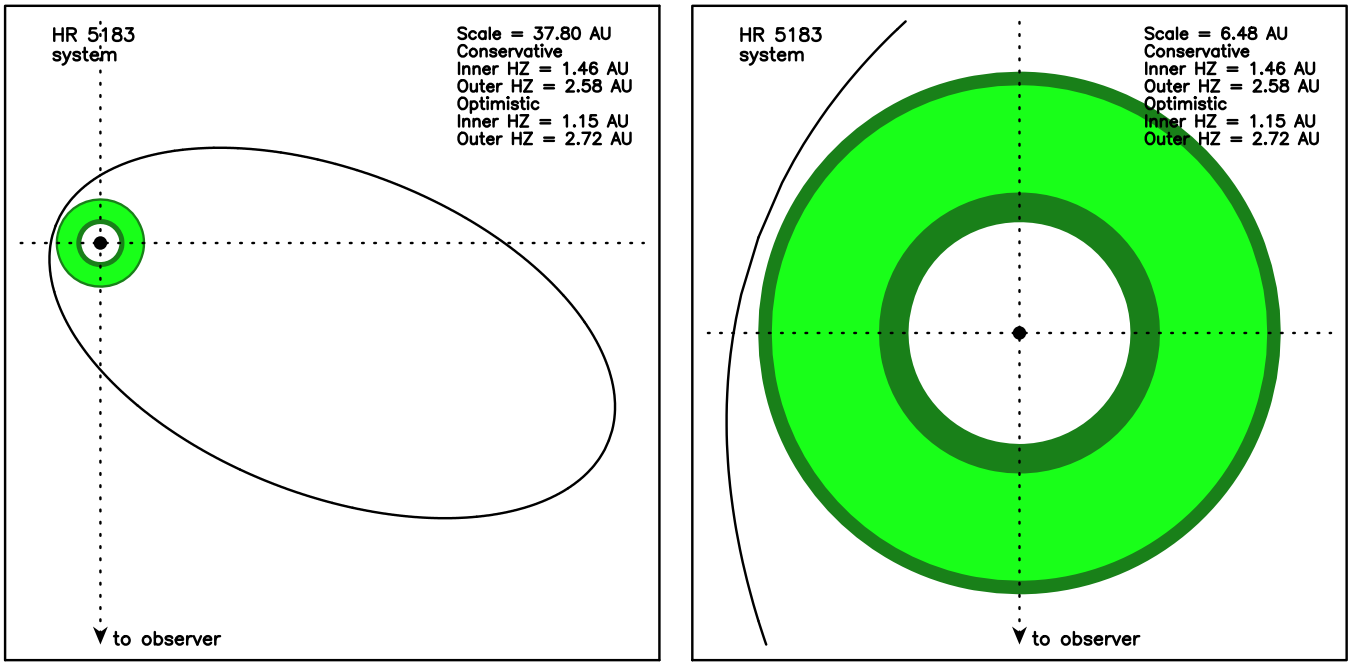

Figure 1. Top–down view of the HR 5183 system, showing the host star (intersection of the dotted cross-hairs) and the orbit of the known giant planet (solid line). The extent of the HZ is shown in green, where light green is the conservative HZ and dark green is the optimistic extension to the HZ. The left panel includes the entire orbit of HR 5183b relative to the system HZ. The right panel is zoomed in on the HZ and highlights the proximity of the periastron of the planet to the outer edge of the HZ.

periastron and apastron distances of 2.89 and 33.11 au, respectively.

The HZ boundaries are derived from Earth-based climate models that calculate the radiative balance for which surface liquid water is retained, described in detail by Kopparapu et al. (2013, 2014). The conservative HZ region extends from an inner boundary, defined by the occurrence of a runaway greenhouse, to an outer boundary, defined by the location where maximum CO_2 greenhouse occurs (Kane et al. 2016a). Similarly, the optimistic HZ region is an empirical extension to the conservative HZ region based on assumptions regarding the retention of surface liquid water in the Venusian and Martian evolutionary histories (Kane et al. 2016a). Calculation of the HZ boundaries depend sensitively on the stellar parameters (Kane 2014), which we adopt from Blunt et al. (2019). The stellar parameters of $T_{\rm eff} = 5794$ K and $R_\star = 1.53\,R_\odot$ result in a luminosity of $L_\star = 2.37\,L_\odot$. Using these stellar parameters, we calculate conservative HZ boundaries of 1.46 and 2.58 au, and optimistic HZ boundaries of 1.15 au and 2.72 au. Figure 1 shows a top–down view of the HR 5183 system, including the orbit of the known planet and the extent of the HZ. As can be seen in the right panel, the known giant planet almost brushes against the outer edge of the HZ.

The presence of such an extreme planetary orbit likely has an associated turbulent dynamical history. The highest known exoplanet eccentricity is that of $e = 0.97$ for HD 20782b (Jones et al. 2006; Kane et al. 2016b). Several studies have suggested that planet–planet scattering events may be a major contributor to the observed distribution of eccentric exoplanetary orbits (Chatterjee et al. 2008; Ford & Rasio 2008; Carrera et al. 2019). For long-period eccentric planets, close encounters with other stars (such as wide binary companions) may serve as the perturbing influence that contributes the required angular momentum to produce highly eccentric orbits (Kaib et al. 2013). Analysis of ancillary imaging and astrometry data by Blunt et al. (2019) indicate that HR 5183 likely does not have a stellar companion, or at least not one that would significantly influence the orbit of HR 5183b. Therefore a planet–planet scattering scenario is the preferred explanation for the observed eccentricity of HR 5183b.

3. Orbital Stability for Terrestrial Planets

Our dynamical study of the HR 5183 system seeks to locate stable orbits within the HZ, such as has previously been determined for the 70 Virginis (Kane et al. 2015), Kepler-68 (Kane 2015), and HD 47186 (Kopparapu et al. 2009) systems. As shown in those cases, the presence of an eccentric giant planet does not exclude terrestrial planets, and in fact, giant planets likely play a contributing role in the formation of terrestrial planets (Lunine et al. 2011).

To test for coplanar stable terrestrial planet locations within the system, we conducted a suite of simulations that explore 200 evenly spaced semimajor axes in the range of 1.0–3.0 au. This range was chosen to fully encompass the extent of the optimistic HZ of the system (see Section 2). At each of the 200 semimajor axes, we placed an Earth-mass planet at randomized starting positions (mean anomalies). The dynamical simulations were then propagated in time along with the known eccentric giant planet.

Our orbital stability simulations were undertaken using *N*-body integrations with the Mercury Integrator Package (Chambers 1999). The integrations utilized the hybrid symplectic/Bulirsch–Stoer integrator with a Jacobi coordinate system, since that generally provides more accurate results for multi-planet systems (Wisdom & Holman 1991; Wisdom 2006), except in cases of close encounters (Chambers 1999). Because relatively long orbital periods are involved, we ran the simulations for 10^8 yr, commencing at the present epoch and an orbital configuration output every 100 simulation years. Based

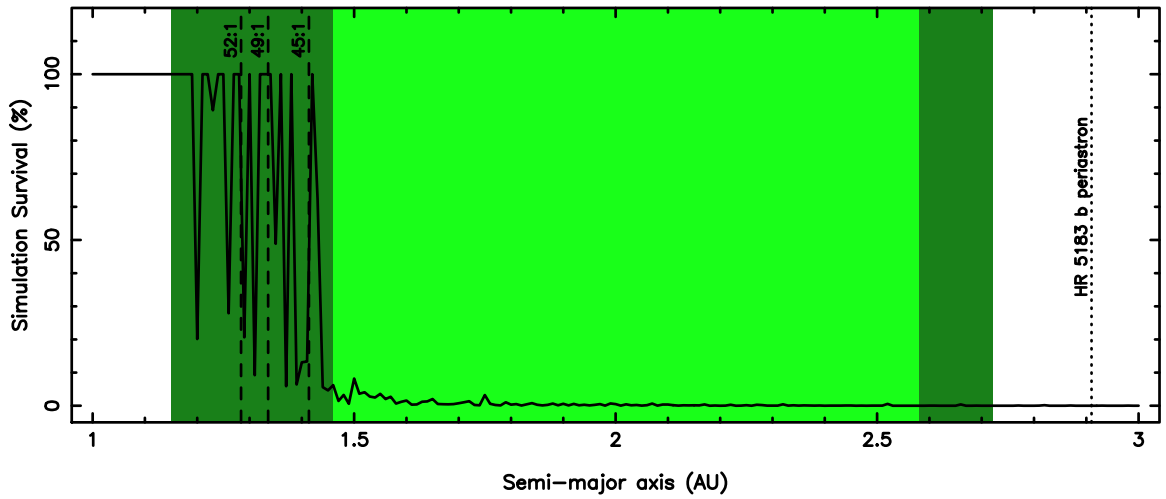

Figure 2. Plot of the dynamical simulation results for an Earth-mass planet located between 1 and 3 au from the host star, represented as the percentage survival of the simulation as a function of semimajor axis (solid line). As in Figure 1, the conservative HZ is shown in light green and the optimistic extension to the HZ is shown in dark green. The periastron passage of HR 5183b is indicated by the vertical dotted line.

on the recommendations of Duncan et al. (1998), a time resolution of 1.0 day was used to meet the minimum required resolution of 1/20 of the shortest orbital period within the system. The orbit of the terrestrial planet is considered stable if it is able to retain its orbital integrity for the duration of the simulation (i.e., neither ejected from the system nor lost to the potential well of the host star).

The results of the dynamical simulations are summarized in Figure 2. At each of the test locations (semimajor axes) for the terrestrial planet, the percentage of the simulations that survived the full 10^8 yr are plotted. The solid line thus indicates the stability of terrestrial planets as a function of semimajor axis. As in Figure 1, the conservative HZ is shown in light green and the optimistic extension to the HZ is shown in dark green. The vertical dotted line at the right of the figure indicates the periastron location of HR 5183b, and thus represents the closest approach of the outer planet to the HZ. As can be seen from the figure, the wrecking ball nature of the giant planet has a devastating effect on the terrestrial planet stability regime, rendering vast swathes of the HZ unstable. The bastion of hope for HZ planets within the system lies within the inner optimistic HZ region, where islands of stability reside. Some of these stability islands may correspond to tenuous resonance locations, indicated by the vertical dashed lines in Figure 2. However, note that planets within the inner optimistic HZ region may be Venus analogs rather than temperate planets (Kane et al. 2014).

A further consideration with regards to stable terrestrial orbits is that terrestrial planets can be significantly more massive than an Earth-mass. The mass ratio of an Earth-mass planet to the mass of the known planet ($3.23\,M_J$) is $\sim 10^{-3}$. Thus it is not expected that a terrestrial planet would significantly influence the orbit of the giant planet. To test the validity of these results for higher mass planets, we repeated the simulations at several specific star–planet separations for a five Earth-mass planet. These simulation results were almost identical to those for the Earth-mass planet simulations, confirming that the stability results presented here apply to a broad range of terrestrial planet masses.

It is worth noting that the uncertainties for the orbital period and semimajor axis of HR 5183b are relatively large. Here we have explored the specific scenario surrounding the maximum likelihood values of these parameters provided by Blunt et al. (2019). The planet has recently passed through periastron passage where the greatest constraints on the orbital solution can be made. Further data past periastron passage over the coming years will allow for an improved precision on the orbital period and subsequent dynamical implications.

4. Predictions of Possible Additional Planets

The possibility of additional planets in the HR 5183 system must satisfy the criteria of being both dynamically stable and beneath the current data analysis detection thresholds. Blunt et al. (2019) adopt a planet injection and recovery technique to determine the sensitivity of their data to additional planets. Their analysis shows that their data are not sensitive to Earth-mass planets and their detection threshold lies at $\sim 30\,M_\oplus$ in the range of 1–3 au. Therefore, the possibility of terrestrial planets within the stable orbit regimes described in Section 3 remains viable.

Here we consider an Earth-mass planet at the largest stable semimajor axis: 1.42 au from the host star. In order to further investigate the orbital integrity at that location, we examined the time-dependent eccentricity of the hypothetical planet, hereafter referred to as planet c. The eccentricity of planet c over the first 10^6 yr of the simulation is plotted in Figure 3. The figure shows that the influence of the outer planet has a dramatic effect on the planet c orbital eccentricity, causing it to vary in the range of 0.0–0.5 with a period of $\sim 10^5$ yr. Furthermore, the high-frequency oscillations present in the eccentricity data match the orbital period of the outer planet. The exchange of angular momentum between two planets resulting in such eccentricity oscillations is typical of systems where the two planets have diverse eccentricities (Kane & Raymond 2014). However, in this case the angular momentum exchange has a significant impact on the eccentricity of planet c while the eccentricity of planet b remains largely unchanged.

A further diagnostic of the eccentricity behavior combined with overall long-term stability lies in the examination of the

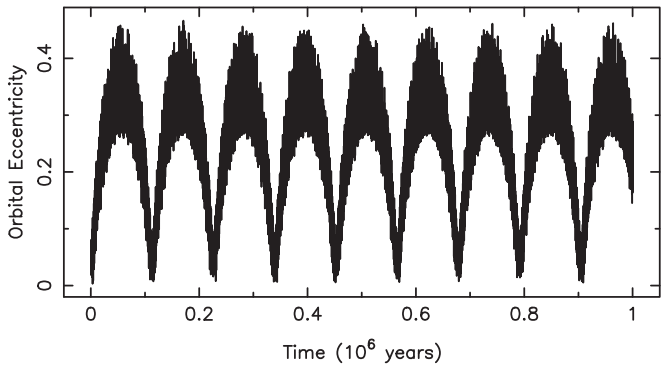

Figure 3. Eccentricity of a hypothetical terrestrial planet located at a semimajor axis of 1.42 au as a function of time for 10^6 simulation years. The plot shows variation of eccentricity in the of range 0.0–0.5 as it exchanges angular momentum with the outer planet.

apsidal mode trajectories. Apsidal motion is generally described as libration or circulation, where the boundary between them is called a secular separatrix (Barnes & Greenberg 2006a, 2006b). Shown in Figure 4 are the apsidal trajectories for planets b and c, represented graphically in polar form. As in Figure 3, the data included are for the first 10^6 yr of the 1.42 au simulation. The data encompass the polar origin and so the planetary system circulates. However, the distance of the apsidal trajectories to the origin is small and so the system is subsequently close to the separatrix boundary between libration and circulation. This proximity to the separatrix explains the relatively high-frequency eccentricity oscillations for planet c observed in Figure 3.

As discussed in Section 1, giant planets within a system may play a significant role in shaping the habitability of terrestrial planets in those systems. As planet b moves through its eccentric orbit, its perturbing influence will undoubtedly scatter material that otherwise would have maintained long-term orbital stability. Many of these perturbed objects will subsequently adopt orbits that make them potential impactors on inner terrestrial planets (Horner & Jones 2008; Georgakarakos et al. 2018). As shown in this section, clearly a major effect of the wrecking ball nature of planet b on HZ terrestrial planets are significant eccentricity variations. For example, the variation in maximum incident flux received at the top of the planetary atmosphere during a complete eccentricity oscillation cycle is represented in Figure 5. At the semimajor axis of 1.42, the planet receives 1.17 times the solar constant ($F_\oplus$), but during periods of high eccentricity, the flux received during periastron rises substantially above the amount of flux received by Venus from the Sun, represented by the dashed line in Figure 5. Similarly, the planet would experience extended periods of relatively low incident flux during the apastron. The effects of orbital eccentricity on planetary climate with respect to habitability have been investigated through the use of both simple and complex climate simulations (Williams & Pollard 2002; Dressing et al. 2010; Kane & Gelino 2012; Way & Georgakarakos 2017). The change in flux received by the planet during periods of high eccentricity would result in eccentricity-driven seasonal effects rather than obliquity-driven seasonal effects (Kane & Torres 2017). However, the thermal inertia of surface liquid water oceans can aid toward a moderation of surface temperature variations and potentially mitigate severe climate effects (Cowan et al. 2012). Even so, the tidal effects caused by extreme eccentricity variations can in some cases lead to runaway greenhouse scenarios resulting from the internal heating of the planet (Barnes et al. 2013).

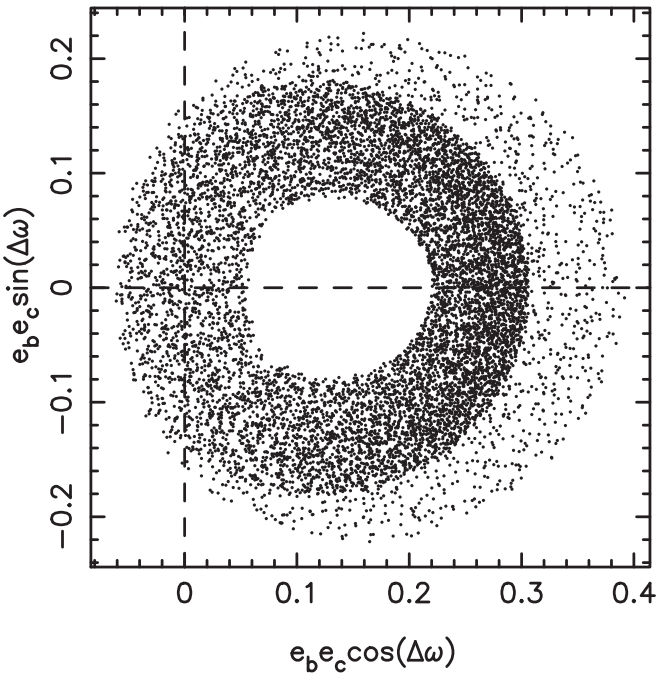

Figure 4. Polar plot of e_b e_c vs. $\Delta\omega$, representing the apsidal trajectory of the b and c planets, where b is the known giant planet and c is a hypothetical terrestrial planet. These data include the first 10^6 yr of the case where planet c is located at 1.42 au from the host star. The figure shows that the apsidal modes are circulating during the dynamical evolution of the simulation, but lie close to the separatrix.

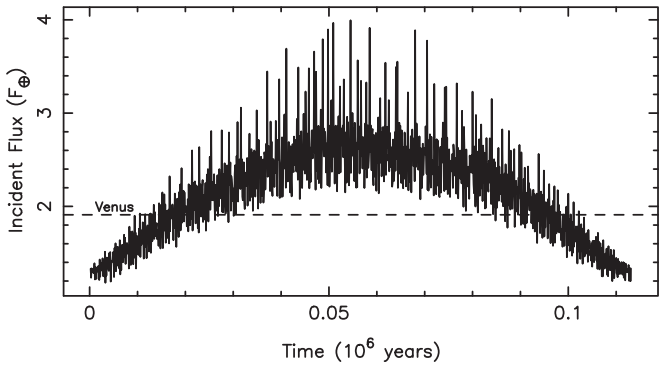

Figure 5. Variation in maximum incident flux received by the planet during one complete oscillation cycle of the eccentricity (see Figure 3) in units of the solar constant ($F_\oplus$). The dashed line indicates the average flux received by Venus from the Sun.

A fascinating aspect of this system to explore is how planet b would appear from the perspective of the hypothetical planet c over the course of a complete orbit of planet b. If such a planet existed in our solar system, the dramatic nature of the observable effects would generally be considered a once-in-a-lifetime event, similar to the perihelion passage of Halley's comet. In Figure 6 we plot the results of our calculations that explore the observable effects as a function of the orbital phase of the outer planet. The top panel shows the distance between the planets assuming that the planets both begin at the minimum separation (inferior conjunction) of 1.47 au. We also assume that this interaction occurs during a period of time where planet c occupies a circular orbit, as shown in Figure 3.

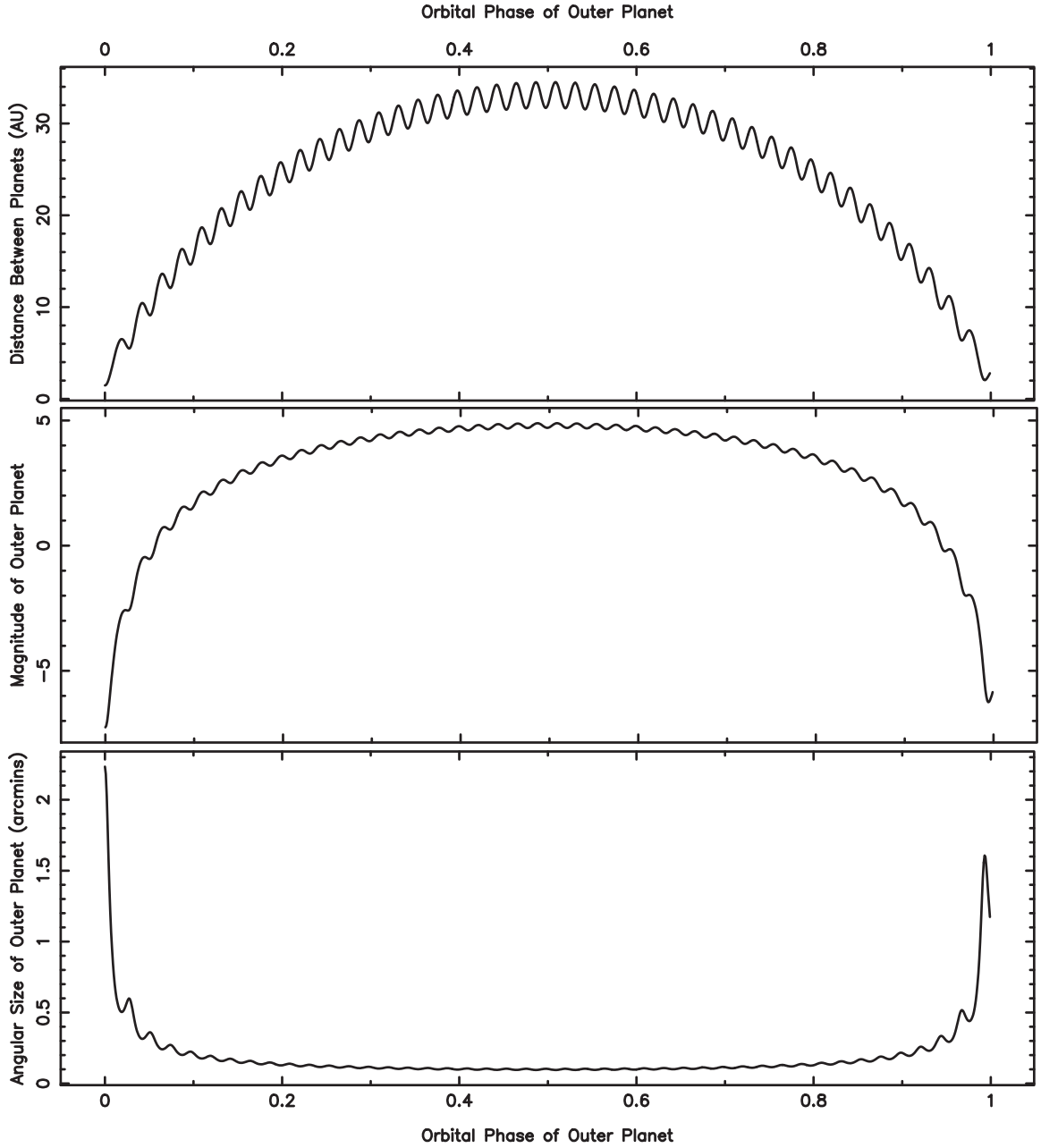

Figure 6. Visibility of the known planet b from the perspective of a hypothetical terrestrial planet located at the farthermost stable orbit of 1.42 au. All panels are shown as a function of the orbital phase of planet b where both of the planets are assumed to start (phase 0.0) at inferior conjunction. Top panel: distance between both planets. Middle panel: visible (*V*-band) magnitude of planet b. Bottom panel: angular size of planet b.

The farthest distance between the two planets (superior conjunction) is 34.5 au. The primary observable effect of the change in distance will be the brightness of the outer planet, depicted in the middle panel of Figure 6, where we have used a Jupiter geometric albedo of 0.538 for planet b. At closest approach, the outer planet will have an apparent visual magnitude of −7.3, 3 mag brighter than Venus and as bright as the 1006 supernova (SN 1006). At its farthest distance, the outer planet has an apparent visual magnitude of 4.9, still visible to the naked eye but fainter than the open cluster M41. Another significant observable change in the appearance of planet b during its orbit would be its angular size, shown in the bottom panel of Figure 6. At closest approach, the angular diameter of the planet will be 2.′2, compared with the 50″ size of Jupiter as seen from Earth during closest approach. This means that an average person on planet c would be able to resolve the size of planet b during the period of closest proximity.

5. Conclusions

One of the primary surprises during the early discovery years of exoplanets was the uncovering of giant planets on highly eccentric orbits. The formation and subsequent orbital evolution of giant planets can follow complex pathways when close encounters significantly perturb the orbital stability of the system. Fortunately, such orbital evolution does not always cause the complete collapse of the system-wide orbital

integrity, allowing other planets to remain in stable orbits even in the presence of highly eccentric giant planets. The discovery of particularly long-period cases, such as HR 5183b, emphasizes the vast diversity of orbital architectures that exist within an array of system formation and outcome scenarios.

The importance of such systems from a planetary habitability perspective arises from a thorough investigation of the dynamical stability of terrestrial planetary orbits, such as the one presented here. The careful analysis of the dynamical integrations demonstrates that planets can survive within a narrow range of locations in the HZ of such systems, even in the presence of a wrecking ball whose orbital origin is likely a chaotic event involving vast exchanges of angular momentum. However, the case of the HR 5183 system also shows that the presence of an eccentric planet will often have a profound effect on the Milankovitch cycles of the HZ terrestrial planetary orbits, causing significant orbital oscillatory behavior. The implications for the climate effects on such worlds may rule out temperate surface conditions, although the stabilizing effects of surface liquid water oceans can also potentially prevent a climate catastrophe. The combination of dynamical simulations, more precise detection techniques, and the characterization of planetary atmospheres, will eventually provide quantitative data to describe the full extent of habitable environments in the presence of giant planets in extreme orbits.

The authors would like to thank Paul Dalba and Michelle Hill for useful feedback on the manuscript. Thanks are also due to the referee, Ravi Kopparapu, for his insightful comments. S. B. is supported by the NSF Graduate Research Fellowship, grant No. DGE1745303. This research has made use of the following archives: the Habitable Zone Gallery at hzgallery.org and the NASA Exoplanet Archive, which is operated by the California Institute of Technology, under contract with the National Aeronautics and Space Administration under the Exoplanet Exploration Program. The results reported herein benefited from collaborations and/or information exchange within NASA's Nexus for Exoplanet System Science (NExSS) research coordination network sponsored by NASA's Science Mission Directorate.

Software: Mercury (Chambers 1999).

ORCID iDs

Stephen R. Kane https://orcid.org/0000-0002-7084-0529
Sarah Blunt https://orcid.org/0000-0002-3199-2888

References

Barnes, R., & Greenberg, R. 2006a, ApJL, 652, L53
Barnes, R., & Greenberg, R. 2006b, ApJ, 638, 478
Barnes, R., Mullins, K., Goldblatt, C., et al. 2013, AsBio, 13, 225
Blunt, S., Endl, M., Weiss, L. M., et al. 2019, AJ, 158, 181
Boisse, I., Pepe, F., Perrier, C., et al. 2012, A&A, 545, A55
Buchhave, L. A., Bitsch, B., Johansen, A., et al. 2018, ApJ, 856, 37
Carrera, D., Davies, M. B., & Johansen, A. 2016, MNRAS, 463, 3226
Carrera, D., Raymond, S. R., & Davies, M. B. 2019, A&A, 629, L7
Chambers, J. E. 1999, MNRAS, 304, 793
Chatterjee, S., Ford, E. B., Matsumura, S., & Rasio, F. A. 2008, ApJ, 686, 580
Cowan, N. B., Voigt, A., & Abbot, D. S. 2012, ApJ, 757, 80
Dressing, C. D., Spiegel, D. S., Scharf, C. A., Menou, K., & Raymond, S. N. 2010, ApJ, 721, 1295
Duncan, M. J., Levison, H. F., & Lee, M. H. 1998, AJ, 116, 2067
Ford, E. B., & Rasio, F. A. 2008, ApJ, 686, 621
Georgakarakos, N., Eggl, S., & Dobbs-Dixon, I. 2018, ApJ, 856, 155
Hill, M. L., Kane, S. R., Seperuelo Duarte, E., et al. 2018, ApJ, 860, 67
Horner, J., & Jones, B. W. 2008, IJAsB, 7, 251
Jones, H. R. A., Butler, R. P., Tinney, C. G., et al. 2006, MNRAS, 369, 249
Kaib, N. A., Raymond, S. N., & Duncan, M. 2013, Natur, 493, 381
Kane, S. R. 2014, ApJ, 782, 111
Kane, S. R. 2015, ApJL, 814, L9
Kane, S. R., Boyajian, T. S., Henry, G. W., et al. 2015, ApJ, 806, 60
Kane, S. R., Ciardi, D. R., Gelino, D. M., & von Braun, K. 2012, MNRAS, 425, 757
Kane, S. R., Dalba, P. A., Li, Z., et al. 2019, AJ, 157, 252
Kane, S. R., & Gelino, D. M. 2012, AsBio, 12, 940
Kane, S. R., Hill, M. L., Kasting, J. F., et al. 2016a, ApJ, 830, 1
Kane, S. R., Kopparapu, R. K., & Domagal-Goldman, S. D. 2014, ApJL, 794, L5
Kane, S. R., Meshkat, T., & Turnbull, M. C. 2018, AJ, 156, 267
Kane, S. R., & Raymond, S. N. 2014, ApJ, 784, 104
Kane, S. R., & Torres, S. M. 2017, AJ, 154, 204
Kane, S. R., Wittenmyer, R. A., Hinkel, N. R., et al. 2016b, ApJ, 821, 65
Kipping, D. M. 2013, MNRAS, 434, L51
Kipping, D. M., Torres, G., Henze, C., et al. 2016, ApJ, 820, 112
Kopparapu, R. K., Ramirez, R., Kasting, J. F., et al. 2013, ApJ, 765, 131
Kopparapu, R. K., Ramirez, R. M., SchottelKotte, J., et al. 2014, ApJL, 787, L29
Kopparapu, R. K., Raymond, S. N., & Barnes, R. 2009, ApJL, 695, L181
Lannier, J., Lagrange, A. M., Bonavita, M., et al. 2017, A&A, 603, A54
Lunine, J. I., O'brien, D. P., Raymond, S. N., et al. 2011, ASL, 4, 325
Raymond, S. N. 2006, ApJL, 643, L131
Sánchez, M. B., de Elía, G. C., & Darriba, L. A. 2018, MNRAS, 481, 1281
Way, M. J., & Georgakarakos, N. 2017, ApJL, 835, L1
Williams, D. M., & Pollard, D. 2002, IJAsB, 1, 61
Wisdom, J. 2006, AJ, 131, 2294
Wisdom, J., & Holman, M. 1991, AJ, 102, 1528
Wittenmyer, R. A., Butler, R. P., Tinney, C. G., et al. 2016, ApJ, 819, 28
Wittenmyer, R. A., Tinney, C. G., Horner, J., et al. 2013, PASP, 125, 351
Wittenmyer, R. A., Tinney, C. G., O'Toole, S. J., et al. 2011, ApJ, 727, 102
Wright, J. T., Marcy, G. W., Butler, R. P., et al. 2008, ApJL, 683, L63